Supporting Information

Engineering the interface of cellulose nanocrystals for transient and bioactive iontronics based on protein eutectogels

Saul Carrasco-Saavedra,[a] Luis Alfonso Jiménez-Ortega,[b] Robin Rojas-Alvarez,[a] Blanca E. Millán-Chiu,[a, c] Gerardo A. Fonseca-Hernández,[a] Perla Itzel Alcántara-Llanas,[d] Kaori Sánchez-Carrillo,[a] Francisco J. Flores-Ruiz,[e] José Basilio Heredia,[b] Matías L. Picchio,[f, g] Josué D. Mota-Morales [a,*]

[a] Universidad Nacional Autónoma de México, Centro de Física Aplicada y Tecnología Avanzada, Querétaro, Querétaro 76230, México.

[b] Centro de Investigación en Alimentación y Desarrollo A.C. Culiacán, Sinaloa 80110, México.

[c] SECIHTI- Universidad Nacional Autónoma de México, Centro de Física Aplicada y Tecnología Avanzada, Querétaro, Querétaro 76230, México.

[d] CIDESI: Centro de Ingeniería y Desarrollo Industrial, 76125 Santiago de Querétaro, Querétaro, México

[e] SECIHTI-Instituto de Física, Benemérita Universidad Autónoma de Puebla, Ciudad Universitaria, Puebla 72570, México.

[f] POLYMAT, Department of Mining-Metallurgy Engineering and Materials Science, School of Engineering, University of the Basque Country (UPV/ EHU), Plaza Torres Quevedo 1, 48013 Bilbao, Spain.

[g] IKERBASQUE, Basque Foundation for Science, Plaza Euskadi 5, 48009 Bilbao, Spain.

*Correspomding author: Josué D. Mota-Morales E-mail: jmota@fata.unam.mx

Figure S1. Typical step height profiles fitted to the cross-section of CNCs crystals.

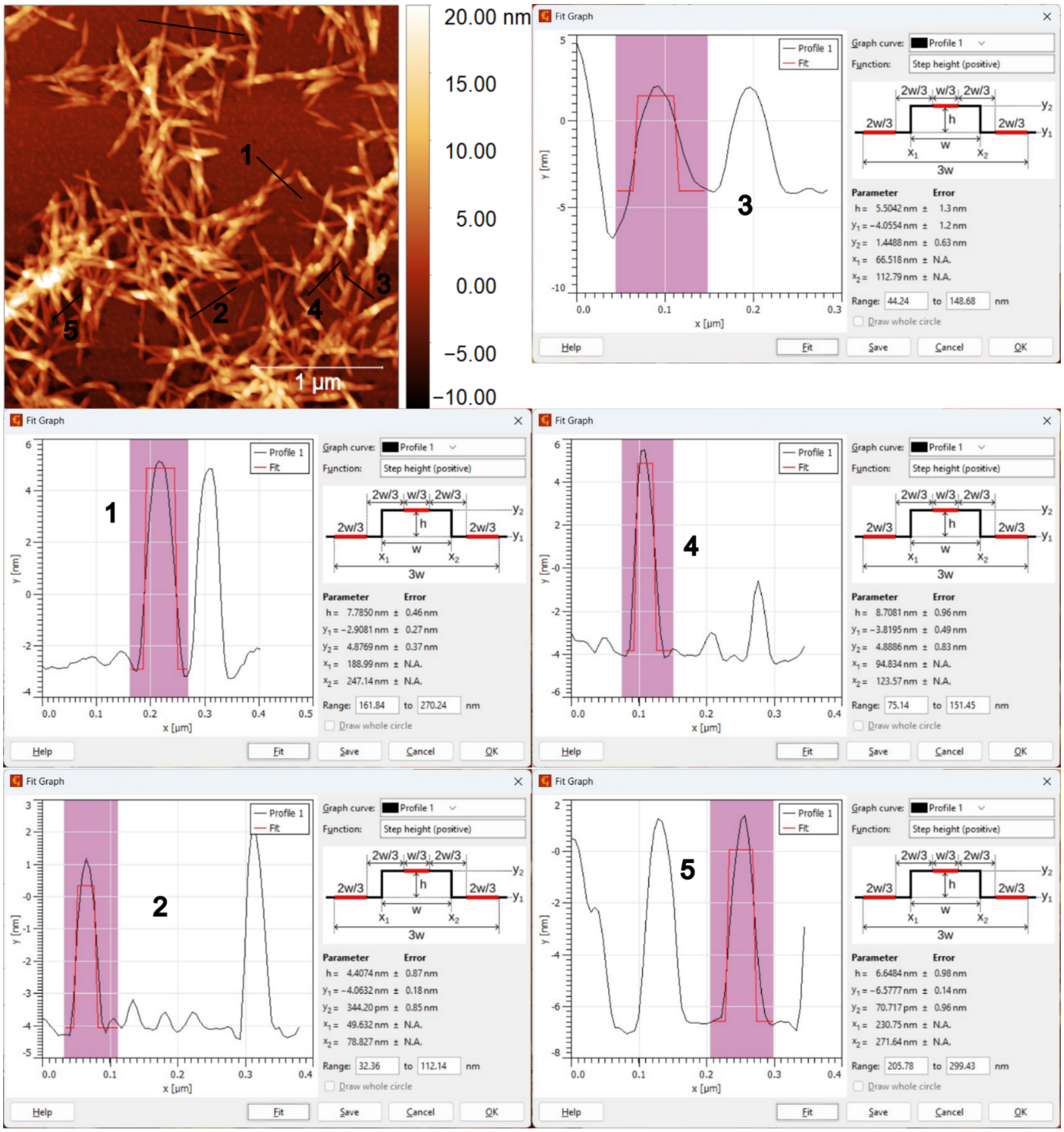

Figure S2. Typical step height profiles fitted to the cross-section of CNC-COOH/TA crystals.

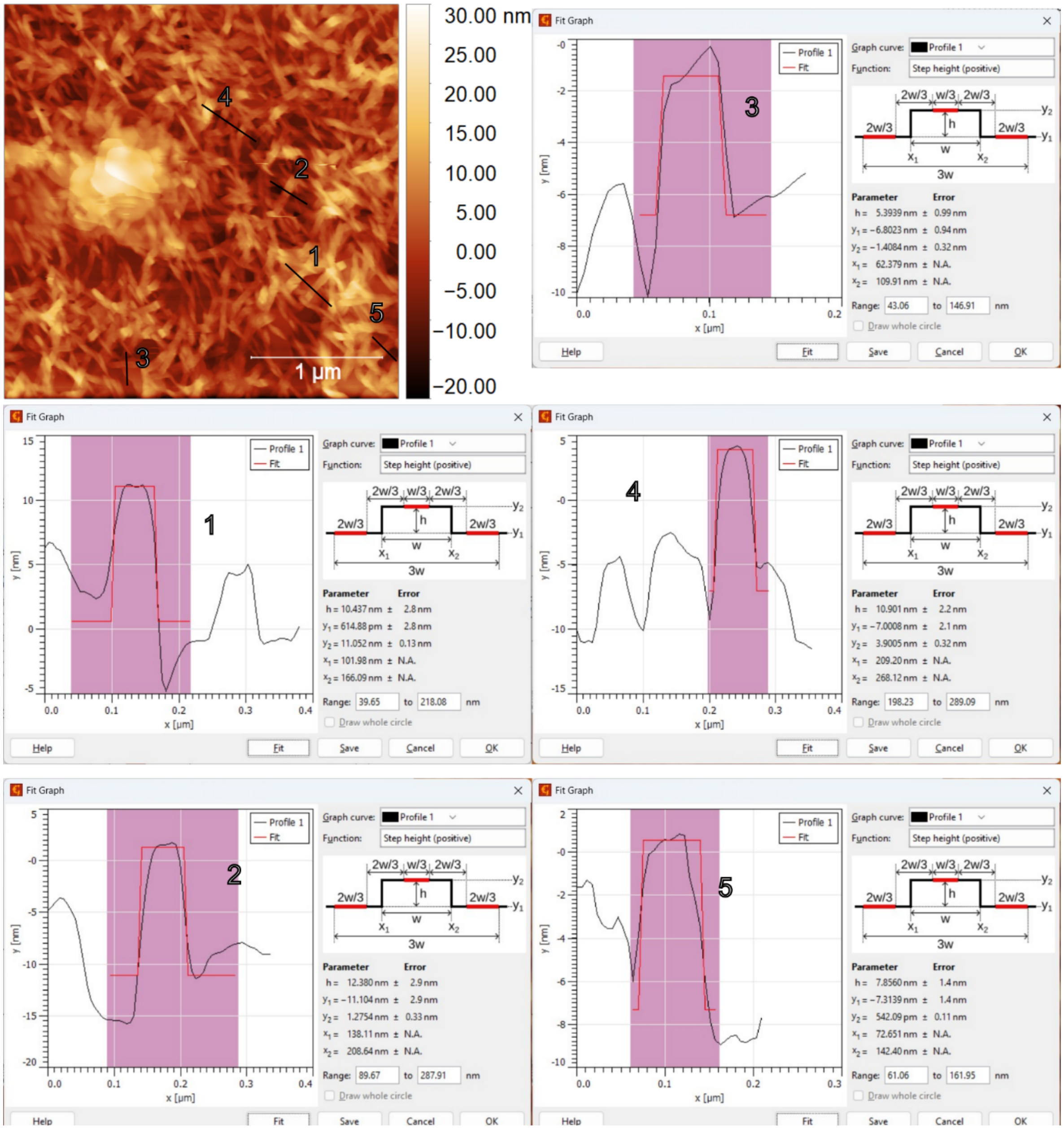

Figure S3. ATR-FTIR spectra of pure gelatin, gelatin eutectogel (22 wt.% gelatin in ChCl-EG DES), and eutectogels nanocomposites containing different concentrations of CNC-COOH/TA.

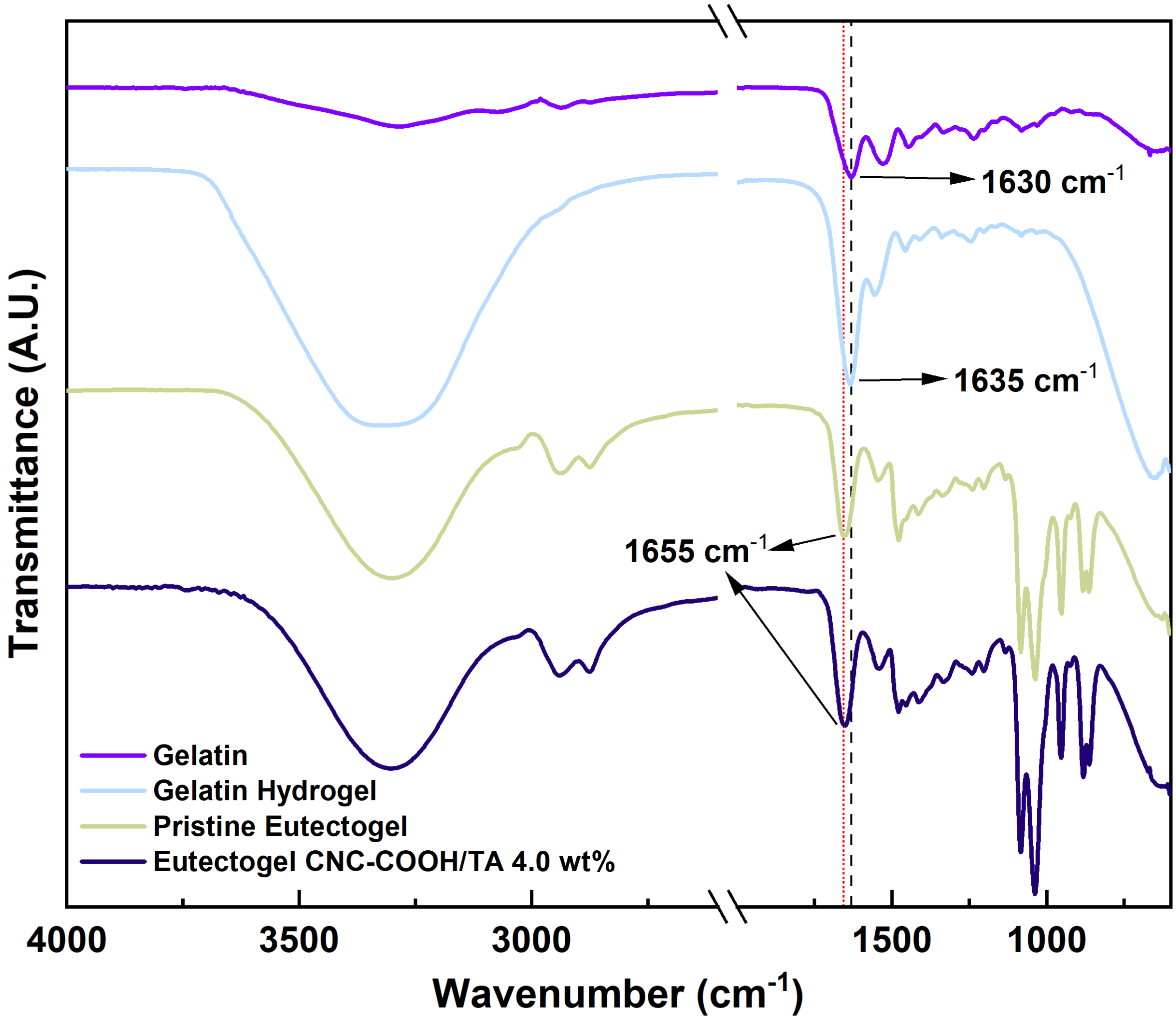

Figure S4. Comparison of tensile stress-strain curves of eutectogel nanocomposites with varying CNC-COOH/TA content and a eutectogel without CNC.

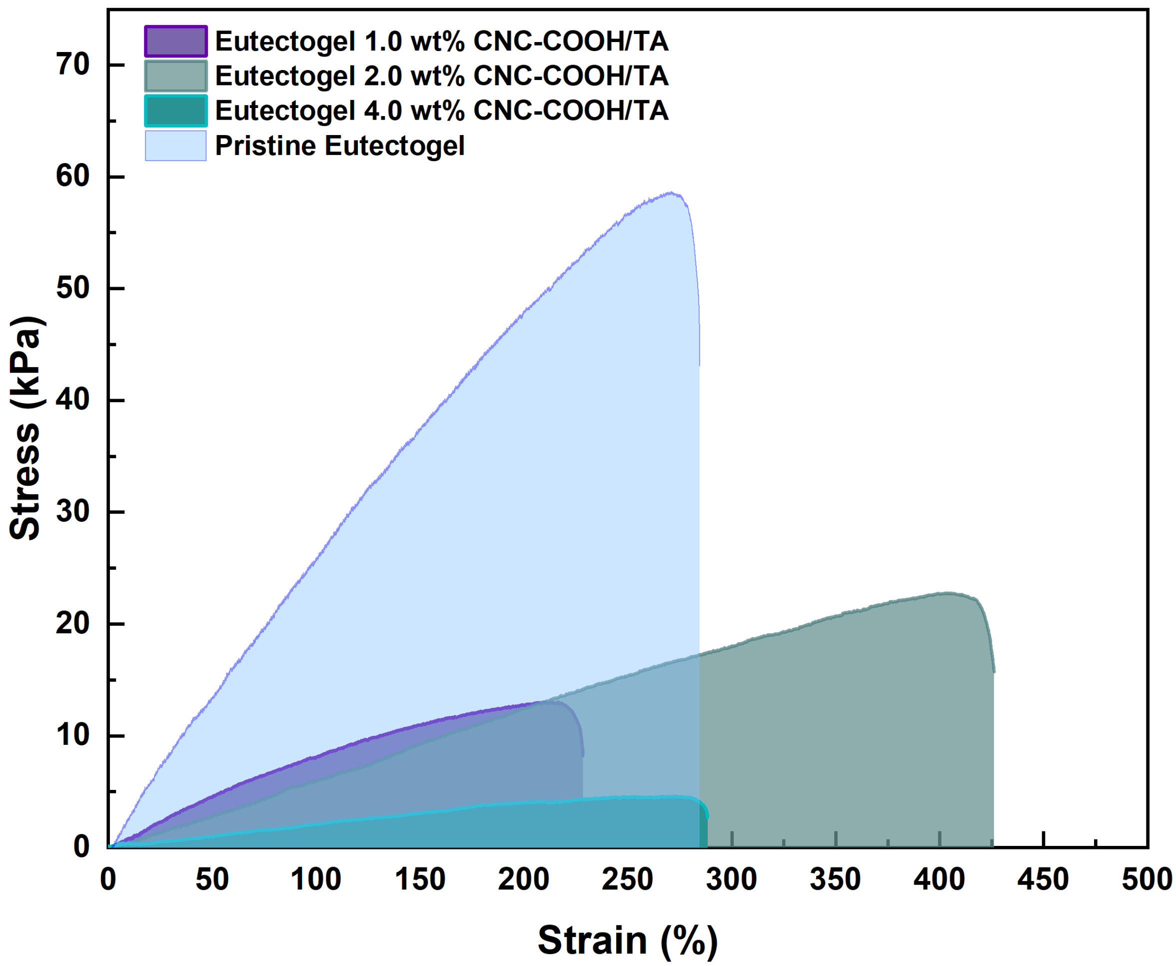

Figure S5. Photographs of the proof-of-concept strain sensor based on the eutectogel nanocomposite and its performance.

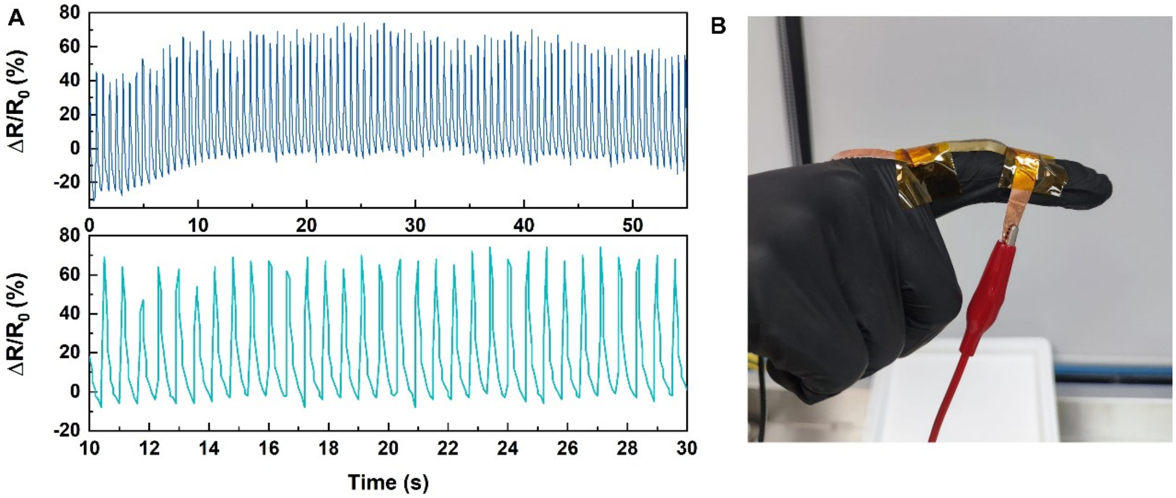

Figure S6. Precipitation of proteins in tryptic soy broth (TSB) upon addition of tannic acid (TA) indicated by the arrow. From right to left: TSB medium, TSB+TA, TSB+DES+TA, TSB+DES

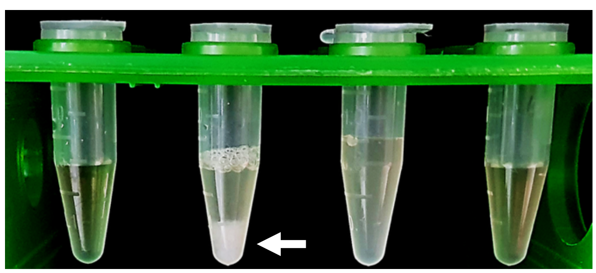

Figure S7. Microplate containing DES (A), and DES-TA (B) in columns 1-10 at different concentrations; column 11 (C+): growth control, column 12 (C-): sterility control. Rows A-C: triplicates of *S. enterica*; row D: control without microorganisms; rows E-F: triplicates of *P. aeruginosa*. Microplate (B) shows evident precipitate formation in column D, whereas in column 1, with the highest DES concentration, the mixture remains stable without precipitate formation. Numbers inside the circles in the bottom row indicate concentrations: molar (M) in panel A and M/mg mL^{-1} in panel B.

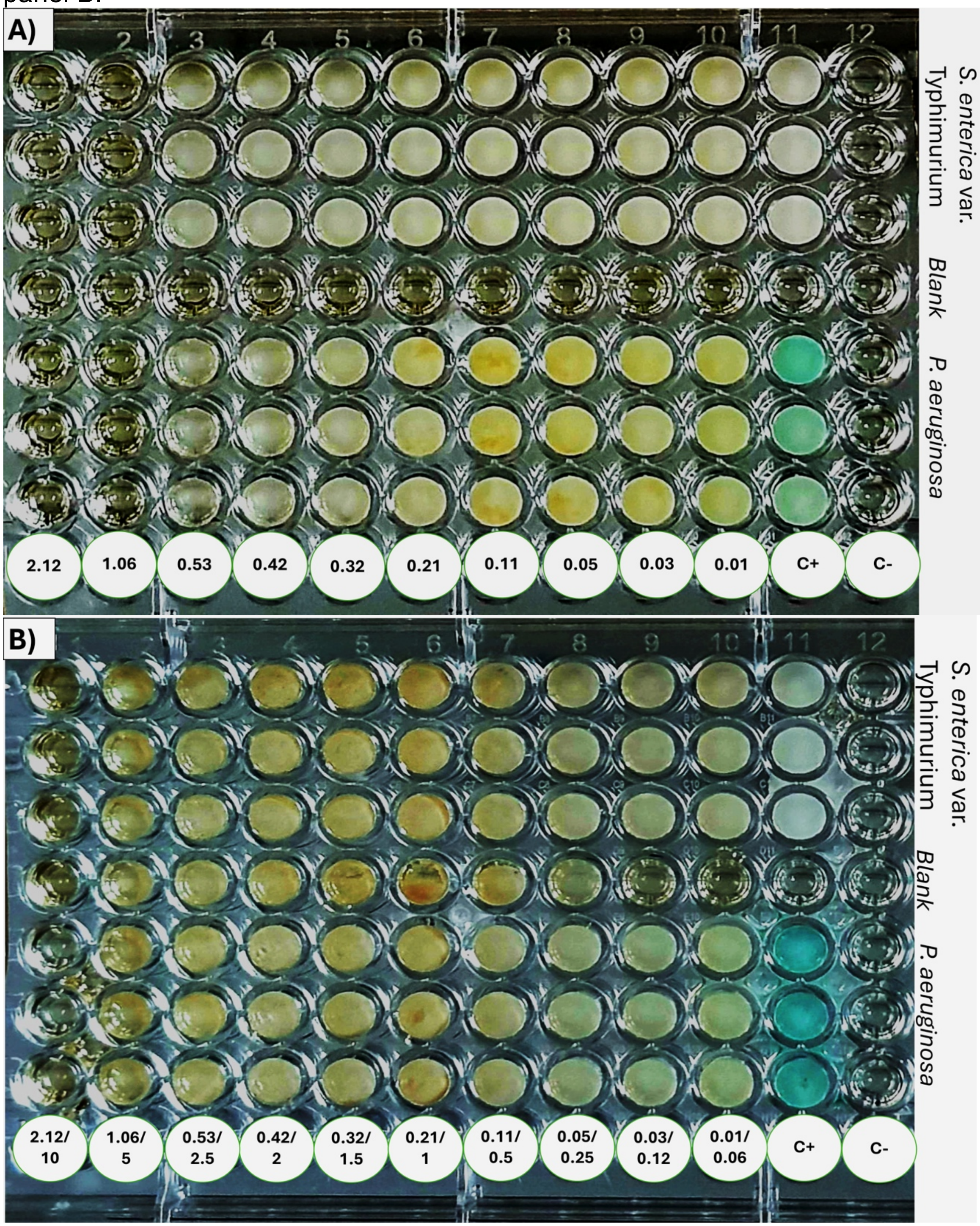

Figure S8. Distribution of ζ- potential of functionalized CNC in water.

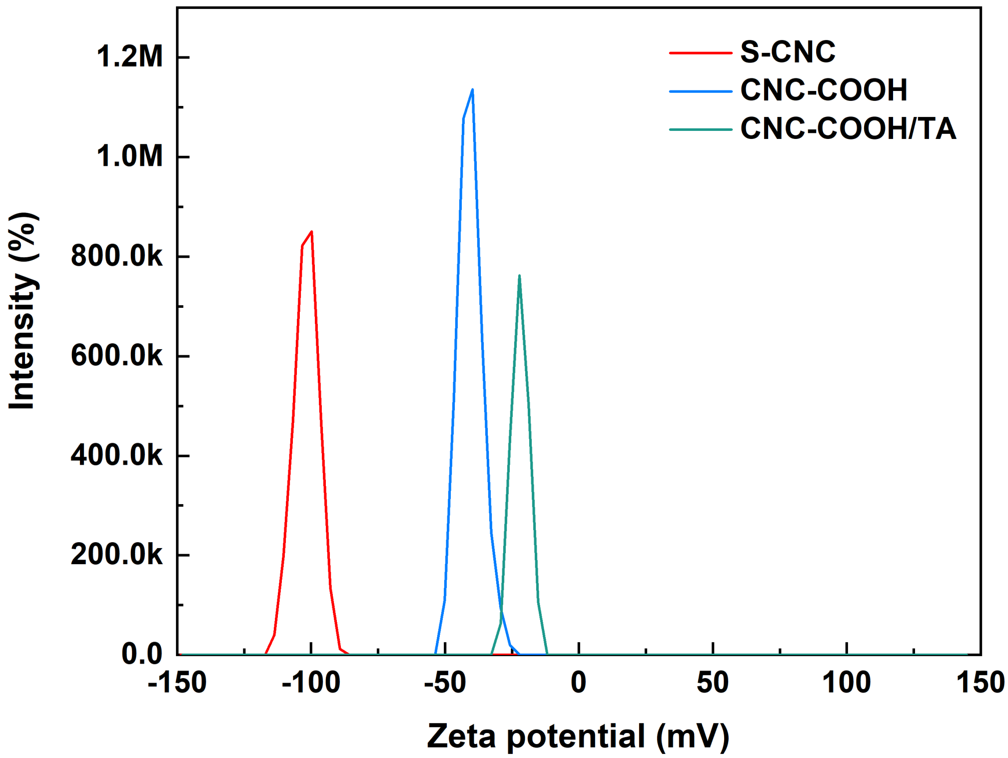

Table S1. ζ- potential of functionalized CNC in water.

Sample	ζ-potential (mV)
S-CNC	-101
CNC-COOH	-40
CNC-COOH/TA	-21

Table shows the ζ- potential values, averaged from three individual measurements per sample. Although S-CNC shows the highest absolute value (100 mV), and can be assumed to be the most stable, due to the sulphonated groups, CNC-COOH and CNC-COOH/TA also present absolute values > 20 mV, thus exhibiting moderate stability. Particularly for CNC-COOH/TA, despite the obtained ζ-potential value, steric stabilization arising from TA-functionalization allows the formation of stable colloids.